Numerical studies on relationship between coda-*Q* and stress field, and prospects for application to real data

Kyosuke OKAMOTO[1], Hitoshi MIKADA[1], Tada-nori GOTO[1] and Junichi TAKEKAWA[1]

[1]Dept. of Civil and Earth Res. Eng., Kyoto University

Coda-*Q* is a stochastic parameter which reflects heterogeneity under the ground. In the past, it is said that the coda-*Q* has a certain relationship with the occurrence of earthquakes or with the change in a stress field. From the perspective that the coda-*Q* has quantitative relationship with the stress field, this study attempts to reveal that relationship using the numerical calculations. A 2-D Finite Difference Method (FDM) and a 2-D Boundary Integral Equation Method (BIEM) are employed to consider the effects of the loaded stress in the crust for two kinds of possible causes. One would be the occurrence of anisotropy in the velocity field, and the other the distribution of crack orientations. The former could be dealt with in FDM, while the other with BIEM. The results suggested that the variation in the coda-*Q* has the relationship with the magnitude of the confining pressure and the angle of principal stress. It is also suggested that both the magnitude of the variation in the coda-*Q* against the confining pressure and against the angle of principal stress shows higher values when the velocity anisotropy is considered. These results imply the possibility to obtain the change in the stress parameters, i.e., both the magnitude and the orientation, using the variation in the coda-*Q*. Our further work will be conducted to apply the present methodology and to confirm the stability of coda-*Q* estimation to real data.

1. Introduction

Coda-*Q* (a kind of *Q* value), obtained from a coda wave, reflects subsurface heterogeneity. In the past, variation of *Q* value against time and space provided stochastic information on subsurface medium in that seismic waves travel through. For example, around volcanoes or immediately before earthquakes show anomalous *Q* values (Matsumoto and Hasegawa, 1989; Got et al., 1990). Also it has been recognized that coda-*Q* and the frequency of earthquake occurrence have a high correlation. This tendency is likely derived from the change of physical properties in the underground due to the loaded stress before earthquakes (Aki, 2004; Hiramatsu et al., 2010). It is fair to say that the stochastic parameter, that is *Q* values, have a certain relationship with physical properties in the underground (Hiramatsu et al., 2000; Aki, 2004).

As mentioned above, several studies have focused on the relationship between the stochastic parameters and earthquakes; however there has been no study that tried to relate the stochastic parameters with non-stochastic parameters, or physical parameters in the underground. This is because the *Q* value is influenced by various parameters in the underground, and when the spatial scale of inhomogeneities becomes comparable with seismic wavelength, it becomes very complicated to analyze the *Q* value quantitatively. Generally, the *Q* value does not indicate any deterministic information on location of scatterers, source, boundaries of layers, etc.

The purpose of this study is to relate the coda-*Q* with the non-stochastic parameter, or the loaded stress. This study will lead to verify the hypothesis, mentioned by Aki (2004), "a change in the loaded stress leads to the change in coda-*Q*" and develop a new monitoring method, which is useful to get the information of stress on site i.e. tunnel drilling, carbon sequestration, etc.

2. Method and Results

Coda-*Q* (denoted as Q_c, hereafter) is acquired from a coda wave. Assuming that c represents attenuation ratio of amplitude of the coda-wave against time, value of the Q_c is obtained by Eq.1.

$$Q = \frac{\omega}{2c} \qquad (1)$$

where ω is angular frequency. Using Eq.1, we obtain the Q_c from the coda-wave calculated by the numerical methods, explained in the following chapters. As seen in Eq.1, behavior of the Q_c^{-1} (reciprocal of the Q_c) is proportional with attenuation ratio c.

(1) Effect of anisotropy of elastic velocity on the coda-Q

Using the FDM, we examined the effect of the velocity anisotropy, which is induced by the loaded stress, on the Q_c^{-1}. We use a staggered grid to discrete the equations of motion (Eq.2) and equations of stress-strain relation (Eq.3 and 4).

$$\rho \frac{\partial^2 u_y}{\partial t^2} = \frac{\partial \tau_{xy}}{\partial x} + \frac{\partial \tau_{yz}}{\partial z} \qquad (2)$$

$$\tau_{xy} = \mu \frac{\partial u_y}{\partial x} \qquad (3)$$

$$\tau_{yz} = \mu \frac{\partial u_z}{\partial z} \qquad (4)$$

where ρ is density, u is displacement, τ is stress, λ and μ are Lame's constants, t is time and x and z are space coordinates.

An elastic wave calculated by the FDM comes from arbitrary angle. By this incident wave, scattering wave field is occurred and at each receiver in the model, the wave is recorded and Q_c^{-1} is calculated (Fig.1). Taking the average of each Q_c^{-1}, we obtain the averaged Q_c^{-1} over the model.

Here we consider three loading patterns (Fig.2). In the Reverse pattern compressive stress is loaded
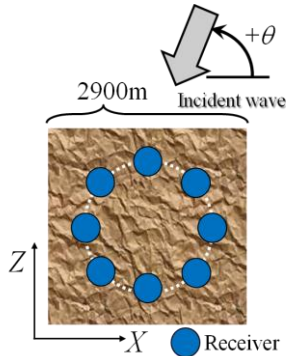

Fig.1 Simulation model for the FDM. $V_s = 5.8 km/sec$, $\rho = 2.6 g/cm^3$. Incident wave is come from arbitrary angle. By the receivers distributed circularly, the set of Q_c^{-1} are obtained.

and confining pressure increases as magnitude of the stress increases. In the Normal pattern tensile stress is loaded and confining pressure decreases. However in the Strike pattern, both compressive and tensile stresses are loaded, so confining pressure does not change. In each case, the Q_c^{-1} is obtained at various magnitudes of the stress from 5 to 50MPa. We assume that the loaded stress closes or opens the cracks selectively according with the equations (Nur, 1971), so that anisotropy on velocity is occurred. Cracks are closed when they satisfy Eq.5 and opened when satisfy Eq.6.
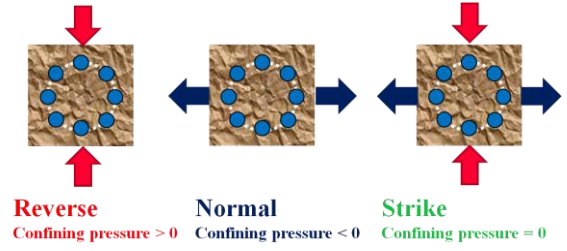
$$\alpha < \frac{\sigma_n}{E} \qquad (5)$$

Fig.2 Three loading patterns are shown. One is Reverse. Other is Normal. The last one is Strike. In each pattern, trend of change in confining pressure (average of the three components of the stress) is different.

$$\alpha > \frac{\sigma_n}{E} \qquad (6)$$

where α is aspect ratio, σ_n is a stress component normal to the cracks and E is Young's modulus.

Fig.3a shows the result of variation of the averaged Q_c^{-1} against magnitude of the stress. From this result, we can say that the averaged Q_c^{-1} is controlled by the confining pressure. In brief when the confining pressure is positive, the greater the absolute value of the stress is, the higher the
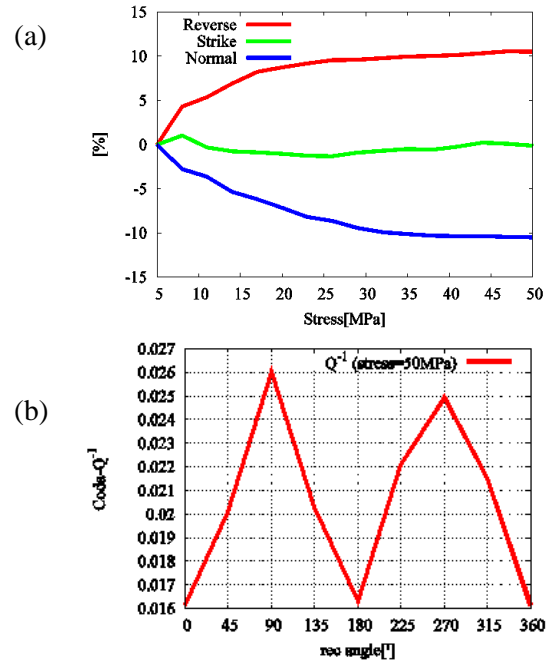

Fig.3 (a) Variations of the averaged Q_c^{-1} at each pattern (Reverse, Strike and Normal) are shown. The vertical axis shows variation of the averaged Q_c^{-1} in percentage and the horizontal axis shows magnitude of the stress. (b) Variation of the averaged Q_c^{-1} against angle of the principal stress. The vertical axis shows magnitude of the averaged Q_c^{-1} and the horizontal axis shows angle of the principal stress.

averaged Q_c^{-1} is marked. On the other hand when the confining pressure is negative, the greater the

absolute value of the stress is, the lower the averaged Q_c^{-1} is marked. As shown in Fig.3, when the both normal and tensile stresses are loaded at the same magnitude, the averaged Q_c^{-1} does not increase or decrease.

We fix the direction of the stress (stress pattern is the Strike) and orientation of the cracks, and then rotate the angle of the incident wave. By this setting angle of the loaded stress is artificially changed. Fig.3b shows variation of the averaged Q_c^{-1} when angle of the principal stress is changed. We can say that the averaged Q_c^{-1} varies periodically according with angle of the stress.

(2) Effect of deflector arrangement of cracks on the Q_c^{-1}

Using the BIEM, a crack is expressed by fictitious sources distributed along its boundary. So the detailed shape and orientation of the crack can be described (see Fig.4). The cracks obey Eq.5 and
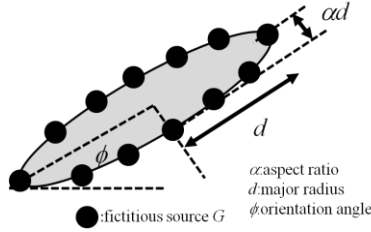
Fig.4 A detailed crack shape is shown. The shape is expressed by fictitious sources. Unlike the FDM, by which the crack is expressed as a point, each crack has a unique shape.

Eq.6. We calculate the effects of change in the orientation and shape of the cracks on the Q_c^{-1}. The simulation model is similar as Fig.1. The difference between the model of the FDM and the BIEM is that each crack has a unique shape in the BIEM. Governing equation for shear wave in the frequency domain is expressed by Eq.7.

$$\mu\left(\frac{\partial^2}{\partial x^2}+\frac{\partial^2}{\partial z^2}\right)G\left(\mathbf{x}_p;\mathbf{x}_s\right)+\rho\omega^2 G\left(\mathbf{x}_p;\mathbf{x}_s\right) \\ =-\delta\left(\mathbf{x}_p-\mathbf{x}_s\right)$$ (7)

where $G(\mathbf{x}_p;\mathbf{x}_s)$ is a Green's function between two locations pointed by two vectors $\mathbf{x}_p$ and $\mathbf{x}_s$ of the form:

$$G\left(\mathbf{x}_p;\mathbf{x}_s\right)=-\frac{i}{4\mu}H_0^{(2)}\left(k\left|\mathbf{x}_p-\mathbf{x}_s\right|\right)$$ (8)

where $H_0^{(2)}$ is the 0th order Hankel function of the second kind and k is the wave number.

We load the stress in the three patterns (see Fig.2). By the loaded stress, the cracks are aligned to a specific direction. Before and after the stress is loaded, the Q_c^{-1} is observed at each receiver and that
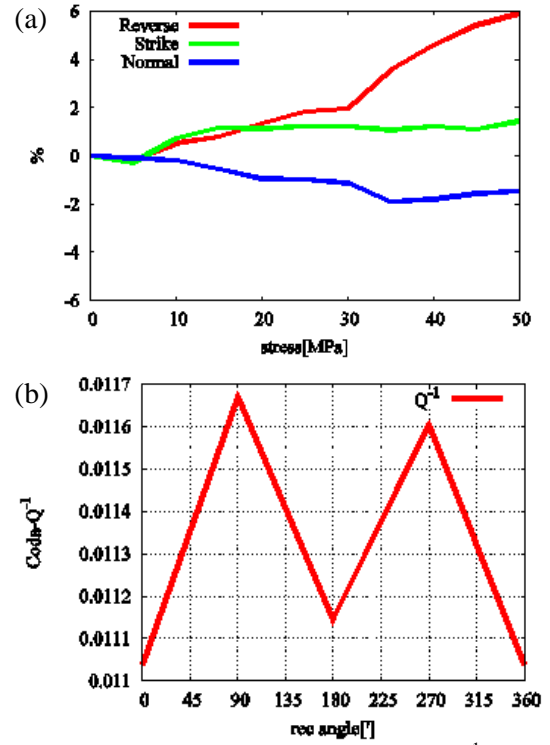
Fig.5 (a) Variations of the averaged Q_c^{-1} at each pattern (Reverse, Strike and Normal) are shown. The vertical axis shows variation of the averaged Q_c^{-1} in percentage and the horizontal axis shows absolute value of the stress. (b) Variation of the averaged Q_c^{-1} against angle of the principal stress. The loading pattern is the Strike (see Fig.2). The vertical axis shows magnitude of the averaged Q_c^{-1} and the horizontal axis shows angle of the principal stress.

Q_c^{-1} is taken averaged over the model. Fig.5a shows the variation of the averaged Q_c^{-1} against absolute value of the confining pressure. The tendency of variation of the Q_c^{-1} is similar as the result of the FDM (see Fig.3). In brief the averaged Q_c^{-1} has relationship with the confining pressure. However the range of that variation is smaller than the variation in the FDM. In the FDM the range of the averaged Q_c^{-1} is about 10% at 50MPa. On the other hand the range in the BIEM is about 5% at 50MPa.

Directional dependence of the averaged Q_c^{-1} is also investigated. Similar to the result of the FDM the averaged Q_c^{-1} varies periodically according with angle of the principal stress (Fig.5b). The range of the averaged Q_c^{-1} in the BIEM is about 5% although the variation in the FDM is more than 10%.

3. Discussion

From the results of the FDM and the BIEM, we can say that there is possibility to know the information on stress field. This is because the averaged Q_c^{-1} has relationship with the confining

pressure and angle of the principal stress. In the FDM the averaged Q_c^{-1} is likely affected by the change in elastic velocity field. The change in the velocity effects on attenuation ratio and it leads to change in the Q_c^{-1}. In the BIEM the averaged Q_c^{-1} is likely affected by the change in density of number of the cracks and angle of the crack. When the number of the cracks or angle of the crack is changed, reflection efficiency of the cracks is changes and it leads to change in the attenuation ratio, and then change in the Q_c^{-1}.

The range of the averaged Q_c^{-1} is larger when the velocity anisotropy is considered (the FDM case) than the BIEM case. This means that the velocity anisotropy caused by loaded stress is major effect which affects to the Q_c^{-1}. Geometric changes like deflection arrangement or change in number of the cracks are minor effect.

4. Future work

To confirm the results of this study, we have started the application of the present method to real data acquired through Hi-net (Okada et al., 2004). For the preparation, we have first examined the stability of Q_c^{-1} acquired from real data.

We chose the Kii Peninsula for the field of study (Fig.6a). The detailed information of earthquakes for the analysis is as follows: epicenters in Wakayama-Hokusei area, the magnitude of earthquakes ranging M2.0-M4.0, the depths of events shallower than 20km, the observation period from June 2002 to June 2011.

Figs.6b and 6c depict the variations of the Q_c^{-1} at Nokami and Hirokawa seismometer stations. It would be fair to say that the error in the estimation of Q_c^{-1} is at most about $\pm 1.0 \times 10^{-4}$. In other words, the variation in Q_c^{-1} corresponds to the change in the stress of $\pm$ 1MPa, according to the above numerical study. Since the stress drop after a microearthquakes in this area generally is 1MPa – 100MPa, we think that it is possible to apply the present method to real data.

REFERENCES
1) Aki, K., 2004, A Perspective on the Engineering Application of Seismology, Proceedings of the7th SEGJ International Symposium, 1-8.
2) Got, J. L., Pouoinet, G., and Frechet, J., 1990, Changes in Source and Site Effects Compared to Coda Q^{-1} Temporal Variations Using Microearthquakes Doublets in California, *Pageoph.*, **134**, 195-228.
3) Hiramatsu, Y., Iwatsuki, K., Ueyama, S., and Iidaka, T., 2010, Spatial variation in shear wave splitting of the upper crust in the zone of inland
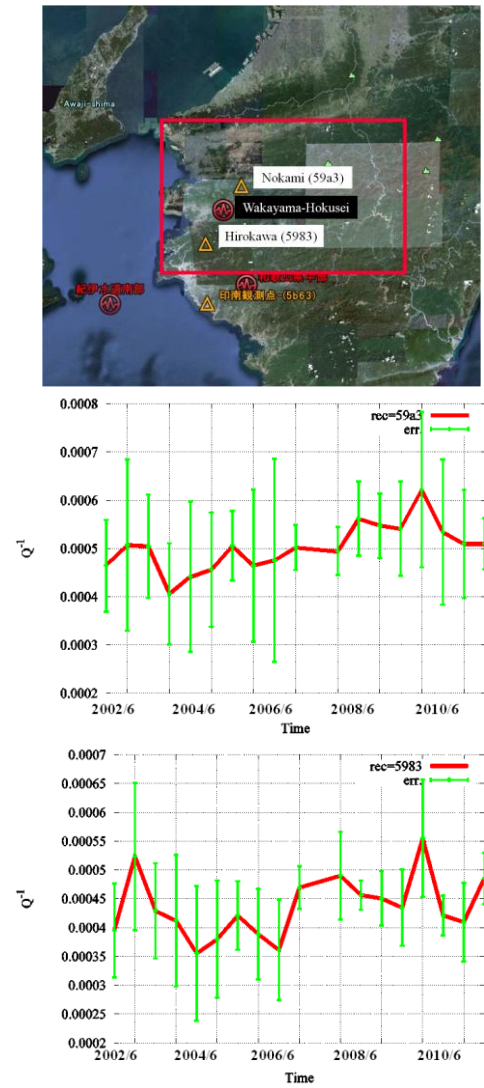
Fig.6 (a) The area we analyze is shown as the red rectangle. (b) Variation of the Q_c^{-1} at Nokami and (c) Hirokawa station are shown.

high strain rate, central Japan, *Eeath Planets Space*, **62**, 675-684.
4) Hiramatsu, Y., Hayashi, N., Furumoto, N., and Katao, H., 2000, Temporal changes in coda Q-1 and b value due to the static stress changes with the 1995 Hyogo-ken Nanbu earthquake, *J. Geophys. Res.*, **105**, 6141-6151.
5) Matsumoto, S., and Hasegawa, A., 1989, Two-dimensional coda Q structure beneath Tohoku, NE Japan, *Geophys. J. Int.*, **99**, 101-108.
6) Nur, A., 1971, Effect of Stress on Velocity Anisotropy in Rocks with Cracks, *J. Geophys. Res.*, **76**, 2022-2034.
7) Okada, Y., Kasahara, K., Hori, S., Obara, K., Sekiguchi, S., Fujiwara, H., and Yamamoto, A., 2004, Recent progress of seismic observation networks in Japan—Hi-net, F-net, K-NET and KiK-net—, *Earth Planets Space*, **56**, 15-28.